ELSEVIER

Polymer 43 (2002) 977–982

polymer

www.elsevier.com/locate/polymer

Molecular dynamics simulation of *cis*-1,4-polybutadiene. 2. Chain motion and origin of the fast process ☆

Okimasa Okada[a], Hidemine Furuya[a,*], Toshiji Kanaya[b]

[a]*Department of Organic and Polymeric Materials, Tokyo Institute of Technology, 2-12-1 Ookayama, Meguro-ku, Tokyo 152-8552, Japan*
[b]*Institute for Chemical Research, Kyoto University, Uji, Kyoto 611-0011, Japan*

Abstract

Molecular dynamics (MD) simulations of *cis*-1,4-polybutadiene in bulk amorphous state were performed to elucidate the origin of a fast relaxation process observed by quasielastic neutron scattering (QENS) measurements. The details of the torsional motion for each dihedral angle were investigated with the torsional auto- and cross-correlation functions for several temperatures in this study. Temperature dependence of the correlation between the torsional autocorrelation and cross-correlation functions is also evaluated. The origin of the fast process of *cis*-1,4-polybutadiene is found to be mainly the cooperative conformational transitions of two dihedral angles located at both sides of the CH_2–CH_2 bond when the bond is in the *trans* conformation. The cooperative conformational transitions exhibit even below the glass transition temperature of *cis*-1,4-polybutadiene. The cooperative motion appears at about 50 K below the glass transition temperature, corresponding to the Vogel–Fulcher temperature. © 2001 Elsevier Science Ltd. All rights reserved.

Keywords: Molecular dynamics simulation; *cis*-1,4-Polybutadiene; Fast process

1. Introduction

The fast relaxation process with a characteristic time of pico second has been observed in the dynamic structure factors (DSFs) and the mean square displacements (MSDs) of hydrogen atoms obtained by the quasielastic neutron scattering (QENS) measurements. This fast process is a characteristic for amorphous materials such as *cis*-1,4-polybutadiene (PB) [1–5], polystyrene (PS) [6,7], polycarbonate [8], *trans*-1,4-polychloroprene [9], poly(vinyl chloride) [10], *ortho*-terphenyl [11–13], and 1-butene [14]. Since the relaxation time of the fast process is independent of both temperature and scattering vectors, it is expected that the origin of the fast process is a very localized motion. For polymeric materials it is reasonable to attribute the origin to the torsional motion. Kanaya et al. [3,5] have suggested that the general feature of the origin of the fast process is the transition in the asymmetric double well potential, corresponding to a C–C torsional potential distorted by the strain of surrounding polymer chains. They have also concluded that the origin of the fast process for PS is assigned to the phenyl ring librational motion [7].

Molecular dynamics (MD) simulation is a powerful tool to investigate the microscopic molecular motion as well as the macroscopic properties. A number of studies have examined the molecular motion and the relaxation processes. Most of them are related to the glass transition phenomena and the molecular motions above the glass transition temperature (T_g). Mattice et al. [15–18] have employed the molecular simulations to investigate the physical properties and the molecular motion of PB. Gee et al. [19] have examined the conformational dynamics using the MD calculations of PB. However, the most of the temperatures, which they have investigated the molecular motion, have been above the T_g. Roe has employed the MD calculations of polyethylene [20,21] and PS [22] for the investigation of the molecular motion with MSDs, intermediate scattering functions (ISFs), and DSFs in a wide temperature range. Van Zon et al. [23] have analyzed the dynamic properties of polybutadiene comparing the mode coupling theory with coherent ISFs obtained by the MD simulations below and above the T_g.

We have analyzed the molecular motion of the *cis*-1,4-polybutadiene in our previous study using the MSDs, ISFs, and DSFs [24]. An onset of a new motion corresponding to the fast process below the T_g was reproduced in the MSD in terms of temperature. The excess intensity in the DSFs below 2 meV above 140 K was also reproduced, which

☆ This paper was originally submitted to *Computational and Theoretical Polymer Science* and received on 29 March 2001: received in revised form on 2 June 2001: accepted on 15 June 2001. Following the incorporation of *Computational and Theoretical Polymer Science* into *Polymer*, this paper was consequently accepted for publication in *Polymer*.

* Corresponding author. Tel.: +81-3-5734-2806; fax: +81-3-5734-2888.
E-mail address: hfuruya@polymer.titech.ac.jp (H. Furuya).

0032-3861/02/$ - see front matter © 2001 Elsevier Science Ltd. All rights reserved.
PII: S0032-3861(01)00629-2

corresponds to the fast process. In this study, the details of the molecular motion were analyzed to examine the origin of the fast process of *cis*-1,4-polybutadiene in bulk amorphous state.

2. Analyses of molecular dynamics calculations

The details of the MD calculations and the force field employed in this study have been described in the previous paper [24]. The methods for the analyses are described in this section. It is reasonable to expect that the origin of the fast process for polymeric materials is related to the torsional motion, since other internal degrees of freedom such as bond stretching and angle bending reside at higher energy regions in DSFs. In amorphous materials it is expected that some atoms are allowed large range movement and some are restricted in small spaces depending on the surroundings. Because of the long chain structure atomic motion is highly restricted in the amorphous polymeric materials. In a short time range the long distance motions are hindered near the T_g and only the torsional motions with a few segments might exist. For this reason we precisely analyzed the dynamic properties for each segment or for each dihedral angle. The molecular motion was investigated mainly with the direct observation of the time evolutions of dihedral angles, the number of the conformational transitions, torsional autocorrelation functions (TACFs), and torsional cross-correlation functions (TCCFs) in this study. The TACF (Eq. (1)) and TCCF (Eq. (2)) at time t for the dihedral angle ϕ_i are defined as [18],

$$G_i^1(t) = \frac{1}{N}\sum g_i^1(t) = \frac{1}{N}\sum \langle \cos(\phi_i(t) - \phi_i(0))\rangle \tag{1}$$

$$G_i^C(j,t) = \frac{1}{N}\sum g_i^C(j,t) = \frac{1}{N}\sum \langle \sin(\phi_i(t) - \phi_i(0))\sin(\phi_{i+j}(t) - \phi_{i+j}(0))\rangle \tag{2}$$

where j represents jth neighbor bonds and the brackets $\langle\ \rangle$ denote the average for all time origins and N is the total number of the corresponding torsional angles. The definitions of the dihedral angles and the segment for the PB chain are shown in Fig. 1. When the TCCFs $G_2^C(j,t)$ for CH_2–CH_2 bond is evaluated, the neighboring bonds are labeled such that the values of j for CH–CH_2 (ϕ_1) and CH_2–CH bond (ϕ_3) are -1 and $+1$, respectively.

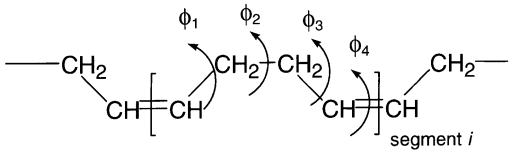

Fig. 1. Definitions of dihedral angles and segment in *cis*-1,4-polybutadiene.

3. Results and discussion

3.1. Torsional autocorrelation functions

The TACFs for the dihedral angles around CH–CH_2 and CH_2–CH_2 bonds of PB at various temperatures are shown in Fig. 2(a) and (b). The torsional motion of the dihedral angles can be examined from the slope of the TACF in the long time region. The negative slopes of TACFs at high temperature indicate that the torsional motion is active and the diffusive motion occurs. Below 170 K the slopes of the TACFs become almost zero suggesting that the torsional motion is inactive and only vibrational motion is taking place. The TACF for CH–CH_2 bonds shows faster initial decay than that for CH_2–CH_2 bonds. The magnitude of the initial decay represents the maximum width of oscillation within torsional potential energy wells. The dihedral angles ϕ_1 and ϕ_3 are expected to have broader potential energy wells than ϕ_2. The features of the TACFs above the T_g are similar to those reported by Kim et al. [17].

The averaged torsional motion is analyzed in Fig. 2 and it seems that the torsional motion is hindered below the T_g. Since the surroundings of each dihedral angle are different from each other and amorphous materials show inhomogenity below the T_g, the distribution for the rotational motion of each dihedral angle is investigated using the TACF. Fig. 3 shows the number of the dihedral angles ϕ_1 and ϕ_3 indicating the value of the TACF for the angle at 10 ps (g_1^1 (10) and g_3^1 (10)) for several temperatures. The insets show the same distributions with different scales in y-axes. At 50 K the values of the TACFs for all the CH–CH_2 bonds are above 0.95, which indicates that the torsional

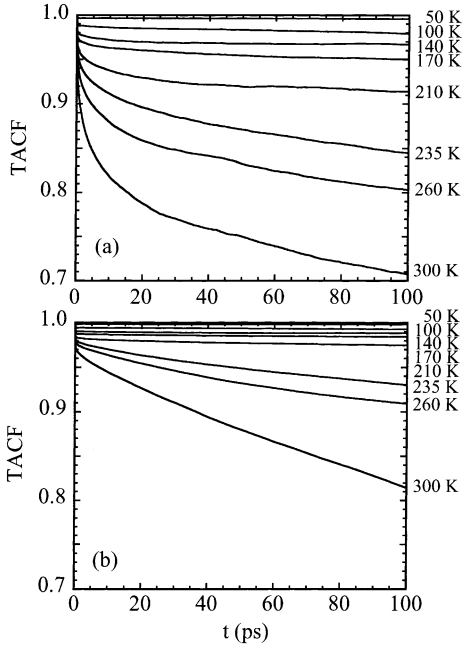

Fig. 2. TACFs $G_i^1(t)$ for several temperatures: (a) CH–CH_2 bond ($i = 1$ and 3), (b) CH_2–CH_2 bond ($i = 2$).

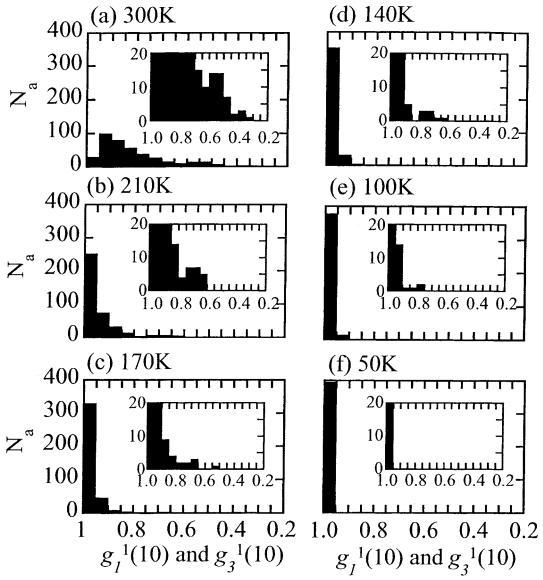

Fig. 3. Distribution of the TACFs for each dihedral angle, $g_1^1(10)$ and $g_3^1(10)$. N_a is the number of the dihedral angle.

motion is restricted. Between 100 and 170 K some dihedral angles have small values of TACFs indicating that the rotational motion occurs. Above 210 K the distribution of the values becomes broad, which implies that the active torsional motion accompanied with conformational transitions occurs frequently.

The temperature dependence for the numbers of the conformational transitions at CH–CH_2 and CH_2–CH_2 bonds are plotted in Fig. 4(a) and (b), respectively. The ranges of the dihedral angles for *anticlinal* conformers A^- and A^+ at CH–CH_2 bonds are from 0 to 170° and from 190 to 360°, respectively. The rotational states at CH_2–CH_2 bonds are defined in terms of the domains of the dihedral angle: T 130/230°, G^- 0/110°, G^+ 250/360°. Since some of the dihedral angles fluctuated around potential barrier tops, the ranges of dihedral angles of 20° without assigned any conformers were set between the defined conformers. A conformational transition is defined as a change in dihedral angle from one region to another. The number of the conformational transitions for CH–CH_2 bonds is much higher than that for CH_2–CH_2 bonds. At 50 K any conformational transitions does not occur for all the bonds. As temperature increases, the number of the conformation transitions gradually increases up to 200 K, which is close to the T_g. Above the T_g the number rapidly increases, which indicates that the diffusive motion occurs. The feature of the curves resembles to the temperature dependence of the MSDs shown in the previous study [24]. That is, three different regions with respect to temperature are observed in both plots. The values of the MSD is proportional to the temperature below 100 K and the values deviate from the line proportional to temperature above 100 K. This implies that in addition to the vibrational motion a new motion starts at around 100 K. Above the T_g the MSD increases dramatically. This similar trend in Fig. 3 shows that the conformational transition might be related to the fast process.

The PB chain is divided into segments including three successive dihedral angles ϕ_1, ϕ_2, and ϕ_3. The average values of $g_i^1(10)$ $(i = 1, 2, 3)$ for dihedral angles in each segment at 10 ps were calculated and classified them into three groups: the ranges of the value for group I, II, and III are 0.70–0.90, 0.90–0.95, and 0.95–1.0, respectively. The ISF and DSF for each group were calculated using the same method shown in the previous study [24]. Fig. 5 shows the

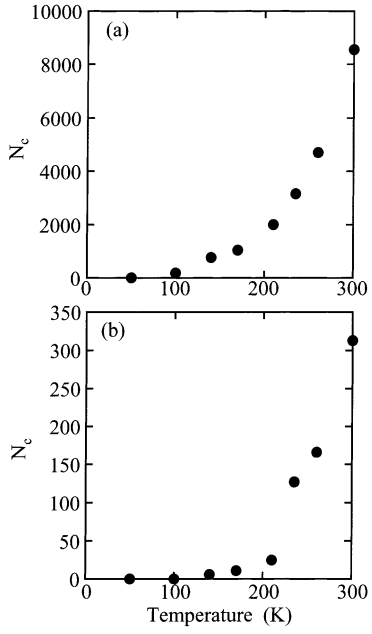

Fig. 4. Temperature dependence of the number of conformational transition (N_c) for each bond: (a) CH–CH_2 bond (ϕ_1 and ϕ_3), (b) CH_2–CH_2 bond (ϕ_2).

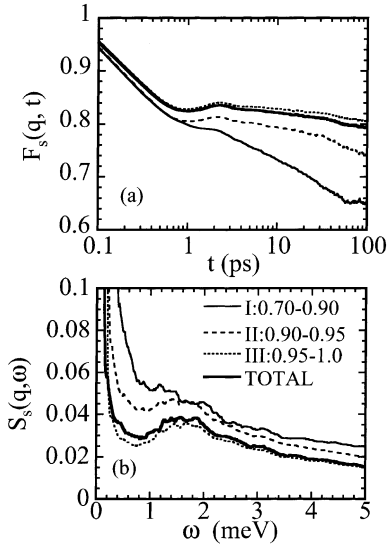

Fig. 5. (a) ISFs and (b) DSFs at 170 K for three groups of the averaged $g_i^1(10)$ $(i = 1, 2, 3)$ values in each segment. Total ISF and DSF are also plotted for comparison.

obtained ISFs and DSFs for the three groups in addition to the total ISF and DSF at 170 K. The DSF for the group I exhibits the excess intensity below 2 meV corresponding to the fast process. In the DSF for the group III, a broad peak assigned to low energy excitation is clearly observed at around 2 meV. The ISF for the group III shows the presence of the 'wiggle' or a momentary reversal of motions at around 1 ps. On the other hand, the ISF for the group I does not indicate the reversal of motions.

3.2. Cooperative torsional motion

The time evolutions of the dihedral angles at several temperatures were traced directly. Some of the conformational transitions are found to be the cooperative motions of counter-rotations between ϕ_1 and ϕ_3, which is represented as

$$A^{\pm}TA^{\mp} \leftrightarrow A^{\mp}TA^{\pm}$$

An example of the cooperative conformational transitions of three successive dihedral angles $\phi_1 - \phi_2 - \phi_3$ at 170 K for 400 ps is shown in Fig. 6. When the dihedral angle ϕ_1 changes its conformation from A^- (120°) to A^+ (240°), the dihedral angle ϕ_3 shifts from A^+ (240°) to A^- (120°) cooperatively at the same moment. The conformation of ϕ_2 is not changed. The schematic feature of this cooperative motion is shown in Fig. 7. Helfand et al. [25,26] have suggested that the conformational transitions in polyethylene occur mostly in pairs of the first and the third of three successive dihedral angles with the central dihedral angle fixed to *trans* conformation. This cooperative conformational transition prevents large movement of two tails, which exist at both sides of the dihedral angle. The detailed features of the cooperative conformational transitions above the T_g have been described by Kim et al. [17]. They have also observed other cooperative motion of three successive dihedral angles $\phi_3 - \phi_4 - \phi_1$ at 300 K, though the cooperativity at ϕ_4 is not as strong

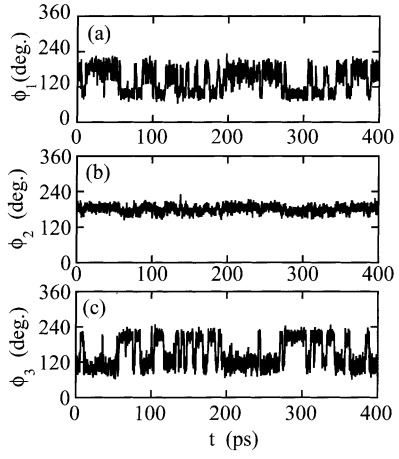

Fig. 6. Time evolutions of three adjacent dihedral angles at 170 K. Cooperative motion of dihedral angles ϕ_1 and ϕ_3 is observed with central dihedral angle ϕ_2 fixed at trans conformation.

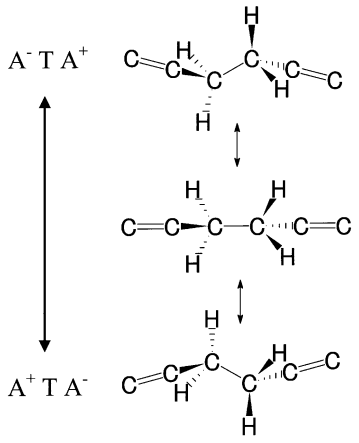

Fig. 7. Schematic representation of the cooperative conformational transition shown in Fig. 6.

as that at ϕ_2 [17]. The cooperative conformational transition of the dihedral angles ϕ_3, ϕ_4 and ϕ_1 is not observed below 170 K in this study, although the existence of the cooperativity is shown in the torsional cross correlation function. Non-cooperative conformational transitions at ϕ_2 are slightly observed down to 140 K. At 100 K the cooperative conformational transitions of the counter-rotation are still observed and the non-cooperative conformational transition is not detected at 100 K. This implies that the potential energy barrier to rotation for this type of cooperative motion is low, which agrees with the suggestion by Helfand et al. [25,26]. At 50 K the conformational transitions are completely ceased and only the vibrational motion in the potential 'cage' is observed.

TCCF was also employed to investigate the cooperative torsional rotation. High cooperativity is observed only for a pair of the dihedral angles ϕ_1 and ϕ_3. Time evolutions of the TCCFs ($j = +2$ and -2) for the second-neighbor dihedral angle pairs at both sides of CH_2–CH_2 and CH=CH bonds are shown in Fig. 8(a) and (b) at 170 and 300 K. The positive value of TCCF indicates the cooperative motion of co-rotation and the negative value indicates that of counter-rotation. A comparison of the TCCFs between $j = -2$ and 2 indicates that two dihedral angle pairs between ϕ_1 and $\phi_3$undergo co- and counter-rotational motions, respectively, and the magnitude of the cooperativity is larger for the angle pair at both sides of CH_2–CH_2 bond than for the pair at both sides of CH=CH bond.

As mentioned above, most of the conformational transitions observed below the T_g are the cooperative motion of three successive dihedral angles $\phi_1 - \phi_2 - \phi_3$ in this simulation. Same as the Fig. 3 for TACF, the values of the TCCF at 10 ps were calculated and the correlation between the values of the TACF and TCCF was evaluated. In Fig. 9, the values of $g_1^C(2,10)$ for the pairs of ϕ_1 and ϕ_3 at 10 ps for all the segments are plotted against the values of $g_1^1(10)$ for the same angle ϕ_1 for various temperatures. Fig. 9(f) indicates that no conformational transition occurs

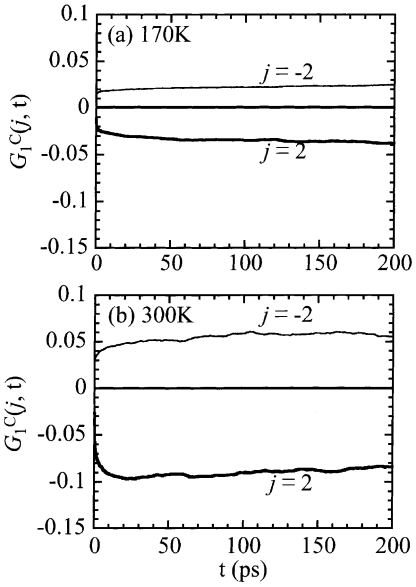

Fig. 8. Torsional cross correlation functions $G_1^C(j,t)$ for ϕ_1 with $j = \pm 2$ at (a) 170 K and (b) 300 K.

at 50 K and the plotted data are concentrated to a small area. As the temperature goes up, the distributions become larger and the plotted data distribute along the line with the slope of 1.0. The cooperative torsional motion enables the large rotation at low temperature. That is, conformational transitions happen only by the cooperative motions at low temperature. At high temperature the plotted data are widely scattered, implying that the bonds with large torsional motion do not necessarily show the large cooperative motion.

3.3. Origin of fast process

In the analyses of the MD calculations of PB we showed that (1) the onset of the fast process above 100 K was confirmed using the MSDs and DSFs, (2) the increase in intensity below 2 meV is related to the torsional motion of the backbone, and (3) the cooperative conformational transitions of the two dihedral angles at both sides of a CH_2–CH_2 bond become dominant below the T_g. These implied that the origin of the fast process is assigned to the cooperative conformational transitions, which begin to occur at around the Vorgel–Fulcher temperature.

In general, particles in amorphous materials are moving with kinetic energy on the potential surface by changing the shape of the potential surface. At high temperature the particles will overcome the barriers to jump from one potential well to another because they have enough kinetic energy. The shape of the potential surface itself will be changed dramatically at the same time, which might cause the diffusive motion. At low temperature the particles are confined in the potential wells created by the surroundings because they do not have enough kinetic energy. However, some particles might overcome the potential barriers to go to the adjacent potential wells by cooperative motion with

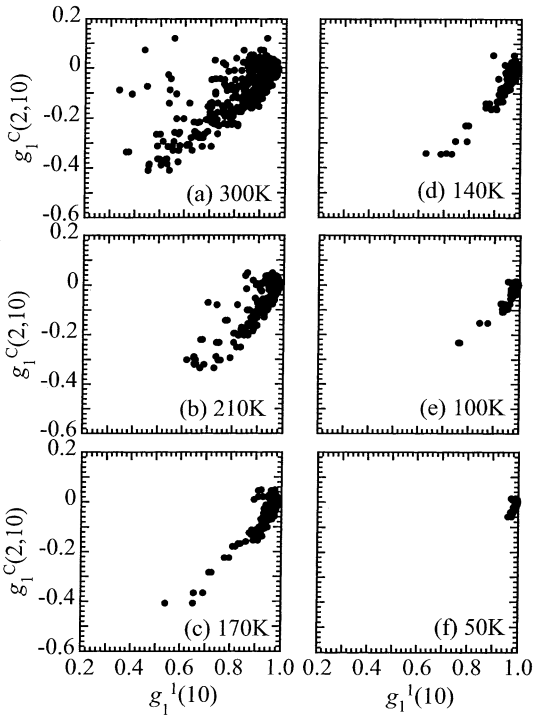

Fig. 9. Correlation between the values of $g_1^C(2,10)$ for the pairs of ϕ_1 and ϕ_3 at 10 ps for all the segments and the values of $g_1^1(10)$ for the same angle ϕ_1 for various temperatures.

other particles, if the barrier is reduced by the cooperative motion. In this MD calculations the cooperative conformational transitions observed below the T_g shown in Fig. 6 are explained as jump motion between the double potential wells expressed by Kanaya et al. [3], where the barriers between the double potential wells in the reaction coordinate would be reduced by the cooperative motion.

We obtained a feature of the torsional motion around the T_g of PB as follows. Above the T_g conformational transitions including the cooperative and non-cooperative rotations occur because the molecules have enough kinetic energy to overcome the barriers for the conformational transitions. As the temperature comes close to the T_g, torsional motion is rapidly suppressed and the frequency of the conformational transitions decreases. Below the T_g the non-cooperative conformational transitions at almost all of the dihedral angles become inactive. The cooperative conformational transitions of the two dihedral angles at both sides of a CH_2–CH_2 bond become dominant, since this type of cooperative motion does not require the large motion of the tails as Helfand has pointed out. Below 100 K, which might correspond to the Vogel–Fulcher temperature in this study, all the conformational transitions are arrested and only vibrational motion in the cage created by the surrounding atoms exists. Our results of MD simulation revealed the relationship between the Vogel–Fulcher temperature and the cooperative motion only for PB chain. Work on other amorphous polymers such as polyisobutylene and poly(methyl methacrylate) is now underway.

4. Conclusion

MD simulations of *cis*-1,4-polybutadiene were performed to elucidate the origin of a fast relaxation process observed above the Vogel–Fulcher temperature by QENS measurements. The details of the torsional motion were investigated with the torsional auto and cross correlation functions at several temperatures in this study. We propose that the origin of the fast process of *cis*-1,4-polybutadiene is mainly the cooperative conformational transitions of two dihedral angles located at both sides of a CH_2–CH_2 bond when the central bond is in the *trans* conformation. This type of motion can be explained by the double potential well model, where the potential energy barrier between the two wells in reaction coordinate are reduced. The feature of the torsional motion above and below the T_g is expressed as follows. Above the glass transition temperature the cooperative as well as non-cooperative conformational transitions are observed. When the temperature of the system is between 100 and 170 K, most of the observed conformational transitions are the cooperative motion. This implies that the Vogel–Fulcher temperature is related to the onset of the cooperative conformational transitions. Below 100 K conformational transitions are completely hindered and only the vibrational motion exists.

Acknowledgements

We also thank Dr S. Kuwajima (Nano Simulation Associates) for permission to use MD code GEMS/MD in our study.

References

[1] Frick B, Richter D, Petry W, Buchenau U. Z Phys 1988;B70:73.
[2] Frick B. Prog Colloid Polym Sci 1989;80:164.
[3] Kanaya T, Kaji K, Inoue K. Macromolecules 1991;24:1826.
[4] Kanaya T, Kawaguchi T, Kaji K. Physica B 1992;182:403.
[5] Kanaya T, Kawaguchi T, Kaji K. J Chem Phys 1993;98:8262.
[6] Frick B, Buchenau U, Richter D. J Colloid Polym Sci 1995;273:413.
[7] Kanaya T, Kawaguchi T, Kaji K. J Chem Phys 1996;104:3841.
[8] Buchenau U, Schönfeld C, Richter D, Kanaya T, Kaji K, Wehrmann R. Phys Rev Lett 1994;73:2344.
[9] Kanaya T, Kawaguchi T, Kaji K. J Chem Phys 1996;105:4342.
[10] Colmenero J. Physica A 1993;201:38.
[11] Frick B. In: Richter D, Springer T, editors. Springer proceedings in physics, vol. 29. Berlin: Springer, 1988. p. 143.
[12] Kiebel M, Bartsch E, Debus O, Fujara F, Petry W, Sillescu H. Phys Rev B 1992;45:10301.
[13] Wuttke J, Kiebel M, Bartsch E, Fujara F, Petry W, Sillescu H. Z Phys 1993;B91:357.
[14] Yamamuro O, Matsuo T, Takeda K, Kanaya T, Kawaguchi T, Kaji K. J Chem Phys 1996;105:732.
[15] Li Y, Mattice WL. Macromolecules 1992;25:4942.
[16] Kim E-G, Misra S, Mattice WL. Macromolecules 1993;26:3424.
[17] Kim E-G, Mattice WL. J Chem Phys 1994;101:6242.
[18] Haliloglu T, Bahar I, Erman B, Kim E-G, Mattice WL. J Chem Phys 1996;104:4828.
[19] Gee RH, Boyd RH. J Chem Phys 1994;101:8028.
[20] Roe RJ. J Chem Phys 1994;100:1610.
[21] Roe RJ. J Non-Cryst Solids 1994;172/174:77.
[22] Roe RJ. J Non-Cryst Solids 1998;235/237:308.
[23] van Zon A, de Leeuw SW. Phys Rev E 1998;58:R4100.
[24] Okada O, Furuya H. Polymer 2002;43:977–982.
[25] Helfand E, Wasserman ZR, Weber TA. Macromolecules 1980;13:526.
[26] Helfand E. Science 1984;226:647.